LA-UR- 02-5829

Approved for public release;
distribution is unlimited.

Title: ELECTROCHEMICAL AND XRD CHARACTERIZATION
OF PLATINUM-RUTHENIUM BLACKS FOR DMFC
ANODES

Author(s): Christian (NMI) Eickes (179516, MST-11), Eric (NMI) Brosha
(109937, MST-11), Fernando (NMI) Garzon (102961,
MST-11), Gerie (NMI) Purdy (100435, MST-11) and Piotr
(NMI) Zelenay (179516, MST-11)
Takanari (NMI) Morita and David (NMI) Thompsett
Fuel Cell Research, Johnson Matthey Technology Centre,
Reading, RG4 9NH, UK

3 9338 01038 9046
LOS ALAMOS NATIONAL LABORATORY

• Los Alamos
NATIONAL LABORATORY

37

ELECTROCHEMICAL AND XRD CHARACTERIZATION OF Pt-Ru BLACKS FOR DMFC ANODES

Christian Eickes, Eric Brosha, Fernando Garzon, Gerie Purdy and Piotr Zelenay
Materials Science and Technology Division (MST-11)
Los Alamos National Laboratory, Los Alamos, New Mexico 87545, USA

Takanari Morita and David Thompsett
Fuel Cell Research, Johnson Matthey Technology Centre, Reading, RG4 9NH, UK

ABSTRACT

It is generally accepted that Pt-Ru alloy catalysts with an atomic Pt-to-Ru ratio of 1:1 generate the best anode performance in the direct methanol fuel cell (DMFC). However, at near-ambient cell operating temperatures, Gasteiger et al. [1] reported that a catalyst with significantly lower Ru content, ~10 at %, offers the highest activity towards methanol. Recently, Dinh et al. [2] demonstrated that the activity of different Pt-Ru catalysts with the same Pt-to-Ru atomic ratio in the bulk might vary depending on the actual surface composition, which is often significantly different from that in the bulk phase. In this work, we study several experimental Pt-Ru catalysts (Johnson Matthey) with Pt-to-Ru atomic ratio ranging from 9:1 to 1:2. Electrocatalytic activity of these catalysts in methanol oxidation reaction is investigated in a regular DMFC and probed using voltammetric stripping of surface CO.

INTRODUCTION

Direct methanol fuel cells (DMFCs) are generally perceived as the most promising fuel cells for portable power applications at low temperatures. The bi-functional mechanism of methanol oxidation, postulated by Watanabe (e.g. [3]), is universally accepted, with unsupported Pt-Ru alloys remaining the best performing anode catalysts to date. According to the bi-functional mechanism, the methanol molecule is first adsorbed on two or three free Pt sites, before undergoing gradual dehydrogenation to form surface CO. Chemisorbed carbon monoxide, which in the absence of Ru would irreversibly block active Pt sites, is then oxidized to CO_2 by the ruthenium oxide species and removed from the surface. In the final stage of the anodic process, ruthenium oxide (and or hydroxide, hydrous oxide) is rebuilt at the surface in a reaction involving bulk water.

While the above mechanism seems to well describe the oxidation process, it is not yet clear what atomic Pt-to-Ru ratio in the bulk of the alloy leads to the highest activity towards methanol. A bulk Pt-to-Ru atomic ratio of 1:1 is often reported to generate the best anode performance, however, Gasteiger et al. [1] reported that at 25°C a catalyst with a surface concentration of 10 at% Ru exhibits the highest activity. The same authors found that an alloy with 30% Ru atoms on the surface is the most active at a somewhat elevated temperature of 60°C. Iwasita et al. [4] investigated Pt-Ru catalysts prepared by

1

various methods and concluded that alloys with surface composition between 10% and 40% Ru lead to the highest activity in methanol oxidation.

In this paper, we present results from a study involving eight unsupported Pt-Ru catalysts with the atomic Pt-to-Ru ratio ranging from 9:1 to 1:2. The catalyst activity was determined directly under actual DMFC operating conditions in a temperature interval from 40°C to 80°C. The active surface area of the samples was probed with CO chemisorbed from either the gas phase or derived from aqueous solution of MeOH, as in an actual fuel cell. The catalyst morphology and composition were also investigated by the X-ray diffraction (XRD), X-ray fluorescence (XRF) and thermogravimetry (TGA).

EXPERIMENTAL

MEA Preparation and Fuel Cell Testing

Unsupported Pt-Ru anode catalysts were manufactured by Johnson Matthey, specifically for the purpose of this study except for Ru-55, which is a commercial DMFC Pt-Ru catalyst from Johnson Matthey, offered under a name of HiSPEC™ 6000. The cathode catalyst was a commercial unsupported Pt black catalyst (HiSPEC™ 1000, Johnson Matthey). Both the anode and the cathode catalysts were applied directly to the membrane at 60°C, according to the standard membrane-electrode assembly (MEA) fabrication procedure adopted at LANL [2,5]. Each 5-cm^2 MEA was conditioned in a hydrogen-air fuel cell at 80°C for several hours. The H_2-air polarization plots were then recorded, followed by extensive testing in the DMFC operating mode with 1.0 M MeOH at 40°C, 60°C and 80°C. As a part of the DMFC testing, the anode activity was examined directly by recording anode polarization plots. For that purpose, the fuel cell was operated in a driven mode, in which the cathode acted as a hydrogen quasi-reference/counter electrode.

CO and MeOH Stripping

After fuel cell testing, the cell was cooled down to 25°C and the temperature of the gas humidification bottles lowered to 30°C. In the CO-stripping experiments the cathode was fed with hydrogen (0.14 L min^{-1}, 0.76 atm) to work as a quasi-reference/counter electrode. Carbon monoxide was adsorbed from a 99.3 % gaseous CO for 10 minutes and at an anode potential of 0.1 V. In order to remove excess CO from the system, the cell was then purged for 30 minutes with nitrogen gas (1.0 L min^{-1}, 0.76 atm). The electrode potential was maintained at 0.1 V throughout the purging. A cyclic voltammogram (CV) was then recorded from 0.1 V to 0.8 V at a scan rate of 5 mV s^{-1}. The experimental conditions for adsorption and purging were carefully optimized in earlier experiments.

CO was also chemisorbed from 1.0 M MeOH solution, fed to the anode for 60 min at a rate of 2 mL min^{-1}. After the chemisorption, the anode was purged with nitrogen (1.0 L min^{-1}, 0.76 atm) to remove excess methanol. The stripping voltammogram was then recorded at a scan rate of 5 mV min^{-1}, the same as for the stripping of CO chemisorbed from the gas phase. Extending the adsorption time to 180 min led to the same results as those obtained in one-hour experiments.

2

XRD

X-ray diffraction methods were used to characterize the crystal structure, phase purity, degree of alloying, and particle size. The measurements were made with a Siemens D5000 diffractometer fitted with an incident-beam monochrometer. The single crystal Ge (220) provided a monochromatic source of $CuK_{\alpha 1}$ radiation. The operating conditions were 50 kV accelerating voltage and 40 mA of beam current. The analysis of the XRD data was carried out using the SHADOW™ full profile refinement package written by Materials Data Corporation. Full profile or whole-pattern analysis methods model the entire X-ray pattern rather than simply determining the d-spacings from peak maxima. The measured peak profile function was modeled by a convolution of an experimentally-determined instrument function and a Lorentzian peak profile sample function. The average crystallite size of the catalyst powder was determined using a Scherrer crystallite size broadening model after de-convoluting the sample profile from the instrument function. Full-profile refinement also yielded FCC unit cell size. The degree of alloying was thus determined by measurement of the d-spacing in the (111) plane of the unit cell. The measured $d_{(111)}$ spacings of the catalyst powders studied in this work were then compared with literature values for Pt-Ru alloys [6]. Vegard's law was used to determine the atomic percentage of alloying.

XRF

A Spectrace QuanX Energy Dispersive X-ray Fluorescence Analyzer (XRF) equipped with a LN_2-cooled Si(Li) detector was used to independently measure the Pt and Ru composition and mass loading. The weight-percentages of Pt and Ru were calculated using a fundamental parameter method included in the QuanX™ analysis software. An advantage of the fundamental parameter method over older empirical standards method is the elimination of the many calibration standards typically required to accurately model a wide range of Pt-Ru stoichiometry. The fundamental parameter method only requires a single calibration standard per element. The XRF cannot detect elements lighter than sodium hence, only Pt to Ru ratios and mass loadings were determined.

Thermogravimetric Analysis

In order to accurately determine the metal content in the samples containing Ru-hydrates, thermogravimetric analysis was used. A Perkin Elmer TGA-7 with flowing forming gas (6% H_2/Ar balance) to reduce the hydrated Ru component to Ru metal was employed. The weight percentage of oxygen and water was calculated from the resulting weight loss at 400-500°C.

RESULTS AND DISCUSSION

Before evaluating the anode catalyst activity in a DMFC, it was necessary to make sure that the cathode properties remain the same in all cells tested with different anode catalysts. Since hydrogen oxidation at the anode is very fast compared with the oxygen reduction at the cathode, the cathode performance was determined from the hydrogen-air polarization plots recorded with each cell. Such H_2-air polarization plots from 1.0 V to

0.4 V are shown in **Figure 1** for MEAs with three different anode catalysts and identical cathode in each case. As expected, in spite of different anodes, all three V-i plots are very similar, with slight deviations occurring only in the voltage range, where the cell performance becomes limited by the mass transport. At a "DMFC-relevant" current density of 0.2 A cm^{-2} the cell voltage was measured at 0.85 V in all three cases while at a significantly higher current density of 0.6 A cm^{-2} the cell voltage was 0.7 V, again the same for all cells.

Cathode reproducibility is further demonstrated in **Figure 2,** in which the H$_2$-air performance at 0.7 V is shown for cells with the anodes made from all eight Pt-Ru catalysts investigated in this work. As expected, the recorded cell current is very similar for all eight cells, with the most extreme values being no more than 10% apart.

After conditioning and making sure that a well-defined cathode "reference" has been established, all eight anode catalysts with different Pt-to-Ru atomic ratios were studied under an assumption that changes in the performance of individual cells are only due to differences in the anode activity. **Figure 3** shows polarization plots obtained with three different Pt-Ru catalysts using 1.0 M MeOH anode feed stream at 80°C. The data demonstrate that Ru-55 with an intermediate a bulk Ru content of 55 at% shows better performance than catalysts with either higher (Ru-65, 65 at% Ru) or substantially lower (Ru-09, 9% Ru) content of ruthenium. This comparison is extended over all eight Pt-Ru catalysts and three temperatures in **Figure 4** shows. Based on the current density values at a typical DMFC voltage of 0.5 V, it turns out that, initially, the cell performance improves with increasing Ru-to-Pt ratio. The best performance is obtained with the bulk atomic content of Ru between 50% and 60 %. Further increase in the ruthenium content results in a decrease in the catalyst activity. In spite of previous reports implying that an optimum Pt-to-Ru ratio could depend on the cell operating temperature, especially at near-ambient conditions [1], in this work, the same pattern of catalyst activity was observed at all studied temperatures: 40°C, 60°C and 80°C (Figure 4).

Catalytic activity of a DMFC anode can also be measured directly by recording anode polarization plots in a driven cell configuration, with the fuel cell cathode being used in this case as a hydrogen quasi-reference/counter electrode. Anode polarization plots for the same three different Pt-Ru catalysts as those shown in Figure 3 are given in **Figure 5**. While the DMFC data in Figure 3 were taken "as is", without applying any *iR* correction, the anode performance data in Figure 5 have been *iR*-corrected to allow true comparison of the relative activity of the catalysts. As expected from the DMFC performance shown above, Ru-55 performs considerably better than the catalysts with either lower or higher content of ruthenium. At a potential of 0.35 V, often used for comparing activity of different anode catalysts, the performance of Ru-55 is approximately six times better than that of the other two catalysts. When current density at 0.35 V is plotted at three temperatures as a function of the ruthenium content for all eight catalysts tested **(Figure 6)**, a dependence similar to that already shown in Figure 4 is obtained. This clearly indicates that the earlier observed difference in the DMFC performance (Figure 4) did indeed result from significant differences in the catalytic activity of Pt-Ru towards methanol.

We demonstrate here a strong correlation between the composition of Pt-Ru anode catalyst and its activity in methanol oxidation. The highest catalytic activity has been obtained with samples having bulk atomic content of ruthenium between 50% and 60%.

CO stripping data, peak potential in particular (see below), indicate that the surface concentration of these most active catalysts is close to 30 at% of Ru, in agreement with Gasteiger et al.[1] and Iwasita et al. [4].

CO Stripping

The CO stripping data recorded at 25°C and normalized to the *BET* surface area are shown in **Figure 7**. Stripping from the surface of a catalyst with the lowest content of ruthenium (Ru-09, solid line) results in a narrow peak at 0.45 V and a shoulder at around 0.52 V. They most likely originate from the CO chemisorbed on the Pt-Ru alloy and islands of pure Pt, respectively. CO stripping from Ru-55, the most DMFC-active catalyst tested, gives rise to a much broader peak and, consequently, significantly higher oxidation charge. The onset potential of CO stripping is noticeably lower on Ru-55 than on Ru-09, which reflects its superior activity in methanol oxidation. Unlike Ru-09 and Ru-55, the ruthenium-rich Ru-65 exhibits virtually no activity in CO adsorption.

The dependence of a total CO stripping charge density, Q, on the catalyst composition is shown in **Figure 8** with a solid line. With increasing Ru content, the CO charge initially decreases and later increases reaching maximum at a point corresponding to 55 at% of Ru (Ru-55 catalyst). Interestingly, the CO stripping charge recorded for relatively inactive Ru-09 is high compared with Ru-50 and Ru-55, which are found to much more active towards methanol in a DMFC testing (*cf.* Figure 4 and Figure 8, fine dashed line). However, if the charge ascribed above to CO stripping from pure Pt sites is subtracted from the total stripping charge for Ru-09, the resulting charge of CO stripping from the alloyed part of the Ru-09 decreases quite significantly. The shape of the thus corrected Q_{CO} vs. $x_{Ru,bulk}$ dependence (Figure 8, thick dashed plot) becomes very similar to the plot of j_{AP} vs. $x_{Ru,bulk}$, representing the actual change in the catalyst activity as a function of the catalyst composition (Figure 8, fine dashed line). In other words, there is a direct relationship between the activity of a catalyst and the tendency for the CO to chemisorb on the alloyed part of that catalyst surface. Furthermore, the CO bound to the pure Pt islands represents those surface sites that get fully blocked by CO under DMFC operating conditions. In the absence of Ru sites anywhere near, such Pt-bound CO cannot be removed from the surface at potentials low enough to be practical for the DMFC operation and remains chemisorbed, thereby rendering that part of the surface inactive in the methanol oxidation reaction. Not surprisingly, the contribution of Pt islands to the overall CO stripping charge is more pronounced for catalysts with relatively high Pt content, *e.g.* Ru-09. Such catalysts show poor DMFC performance in spite of a relatively high total CO stripping charge.

Another interesting case is that of Ru-61. In spite of showing high activity towards methanol (Figure 8, dashed line) this catalyst tends not to get significantly covered by the surface CO (Figure 8, thin dashed line). Characteristic of this catalyst is high content of ruthenium oxides (hydroxides) in the bulk, which are not known to adsorb CO to a significant degree (*e.g.*, [7]). XRD evidence that confirms the presence of ruthenium oxides will be shown below in the next section. However, the oxides (hydroxides) may affect the surface the properties of the catalyst, possibly through electronic effects from the layers immediately below the surface layer. Although no explanation of a good DMFC performance of Ru-61 can be given at this time, this case clearly shows the limits of CO stripping as an activity probe for the Pt-Ru anode catalysts.

One way of possibly making the CO probe more relevant to DMFC operation is to generate surface CO from methanol rather than adsorb it from a gas phase. Unlike in the case of CO adsorbed from the gas phase, stripping methanol-generated carbon monoxide is expected to be specific to Pt-sites for it is known that MeOH only adsorbs on platinum and not on ruthenium (*e.g.*, [1, 8]). In this work, the methanol-generated CO was used to determine the nature of the shoulder in CO stripping peaks on Ru-09 and Ru-18. Comparison of the stripping scans of CO formed on Ru-09 from the gas phase and from 1.0 M aqueous MeOH are shown in **Figure 9** with solid line and dashed line, respectively. Based on the comparison of stripping charges and peak locations it becomes immediately clear that the CO-stripping shoulder does indeed arise from the CO stripping from Pt islands. The difference in the CO stripping charge measured on Ru-09 after adsorption form the gas phase and from aqueous solution of methanol is about 70 μC cm^{-2}, *i.e.* close to 30% of the total charge for stripping of the gas-phase CO. Work is in progress to reproducibly correlate the charge difference with surface activity of different unsupported Pt-Ru catalysts towards methanol.

XRD and TGA analysis

In **Figure 10**, the X-ray diffraction pattern is presented for two "as-received" catalysts: Ru-09 and Ru-65. While the low ruthenium content catalyst exhibits sharp diffraction peaks, a pronounced background can be seen for the catalyst with the highest Ru content. This indicates the presence of amorphous Ru oxides and/or hydroxides in the Ru-65 sample. Diffraction peaks belonging to crystalline RuO_2 can also be found in the pattern as shown in Figure 11b. Full-profile fitting of the XRD data show an average crystallite size of 5.2 nm for the Pt-Ru alloy of Ru-09 and 2.9 nm and 1.0 nm for the Pt-Ru alloy and RuO_2, respectively, in the Ru-65 sample. Thermogravimetric analysis (TGA) under reducing conditions (6%H_2/Ar balance) confirms the presence of possible oxides and/or hydroxides. Analysis of the Pt unit cell lattice parameter in the alloy suggests that all samples displayed incomplete alloying; the FCC phase was typically Ru deficient. No HCP phase material was observed in high Ru content samples. These data are summarized in **Table 1**.

Table 1: XRD, XRF and TGA Summary

Catalyst[1]	Ru Content[2] (at%)	Surface Area[3] ($m^2 g^{-1}$)	Average Crystallite[2] Size (nm)	XRF Composition (at%)		TGA Weight Loss (%)
				Pt	Ru	
Ru-09	10	34	5.2	89	11	*n.m.*[4]
Ru-18	10	46	4.3	79	21	*n.m.*
Ru-33	20	61	2.9	63	37	*n.m.*
Ru-50	40	86	1.8	46	54	*n.m.*
Ru-52	35	86	2.0	46	54	10
Ru-55	35	67	1.8	46	54	12
Ru-61	20	115	1.6	35	65	18
Ru-65	15	122	2.9	30	70	20

[1] *Total Ru content determined by "wet chemistry" method;* [2] *XRD data for alloyed Pt-Ru phase only*
[3] *By N_2 BET;* [4] *Not measured*

In spite of vast effort invested into making all eight catalysts well alloyed and therefore differing from one another by only the Pt-to-Ru atomic ratio, the relative content of the Pt-Ru alloy in the samples changes significantly as the ruthenium content increases from as low as 9 at% to as high as 65 at%. Even before completing the ongoing XRD study of the "as-received" samples, there is a strong indication that the catalysts in this study can be divided into two groups: (i) "true" Pt-Ru alloys and (ii) catalysts of the Pt/"$RuO_x \cdot (H_2O)_y$" type, with a relatively low content of the Pt-Ru alloy. More work is currently underway at Los Alamos to better correlate electrocatalytic activity of Pt-Ru catalysts in these two groups with the average particle size, degree of alloying and the content of amorphous Ru oxide/hydrous oxide/hydroxide. Also, to make XRD data as relevant as possible to the actual DMFC operating conditions, X-ray diffraction experiments with reduced catalyst samples will be carried out.

CONCLUSIONS

It is very difficult to prepare a series of Pt-Ru alloys with differing atomic ratios while maintaining similar crystallite sizes, surface areas and phase homogeneity. Comprehensive catalyst materials analysis is required for all samples before conclusions can be drawn about what factors influence anode catalytic activity. For our series the optimum bulk composition of a binary Pt-Ru catalyst for methanol oxidation at the DMFC anode is between 50 and 60 at% of Ru, which typically corresponds to ~30 at% of Ru on the surface. The best-performing catalyst composition is temperature independent in the temperature range investigated in this work, from 40°C to 80°C.

The stripping charge of carbon monoxide chemisorbed from the gas phase or from an aqueous solution of methanol gives an indication of the catalyst activity, yet it can only be used as a first approximation of the total number of free catalyst sites available to methanol oxidation. Stripping of a methanol-derived CO appears to be an effective tool for identifying two different adsorption sites for catalysts with high Pt content, namely, Pt-Ru alloy sites and pure Pt islands.
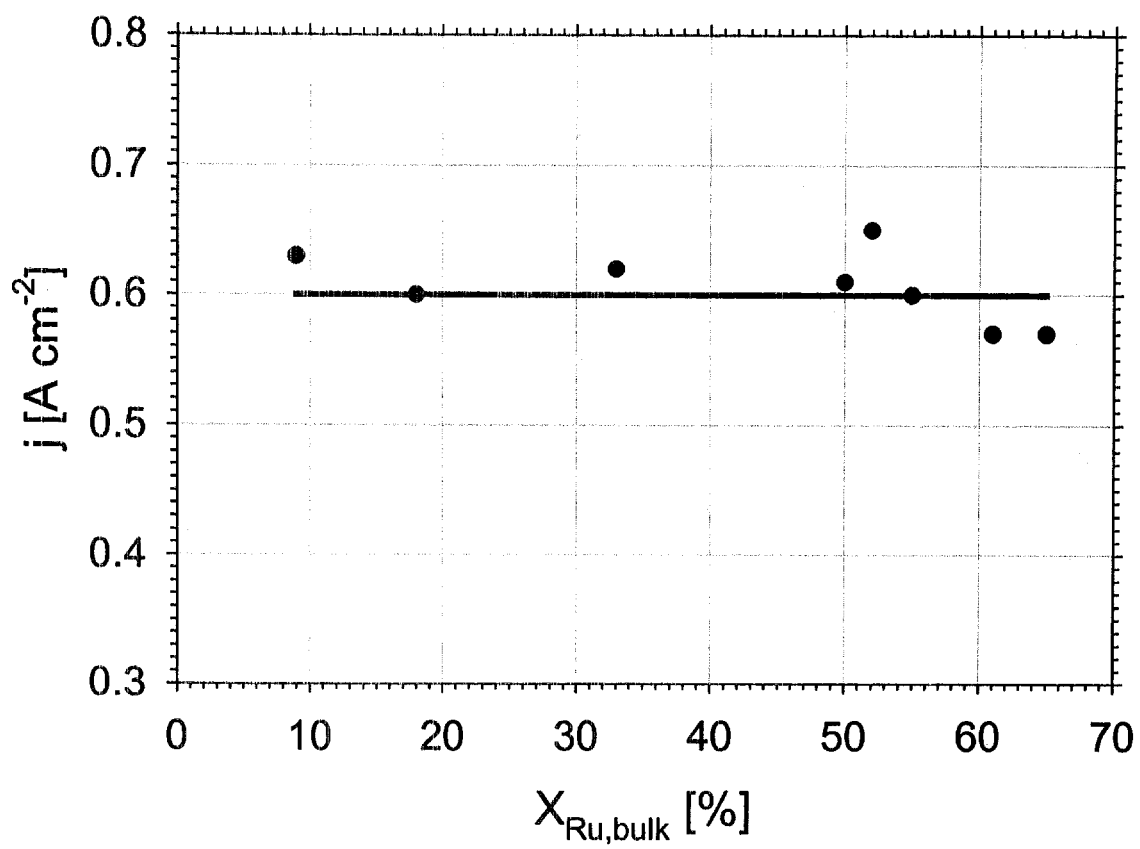
ACKNOWLEDGMENTS
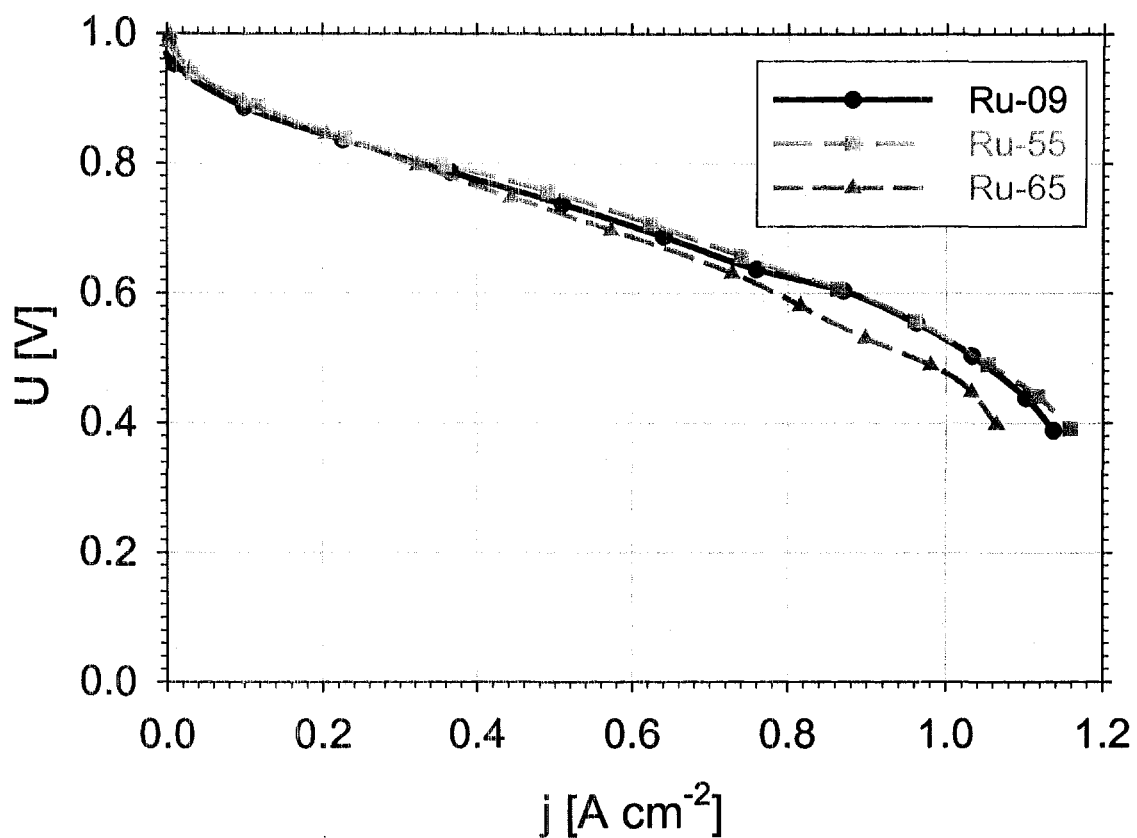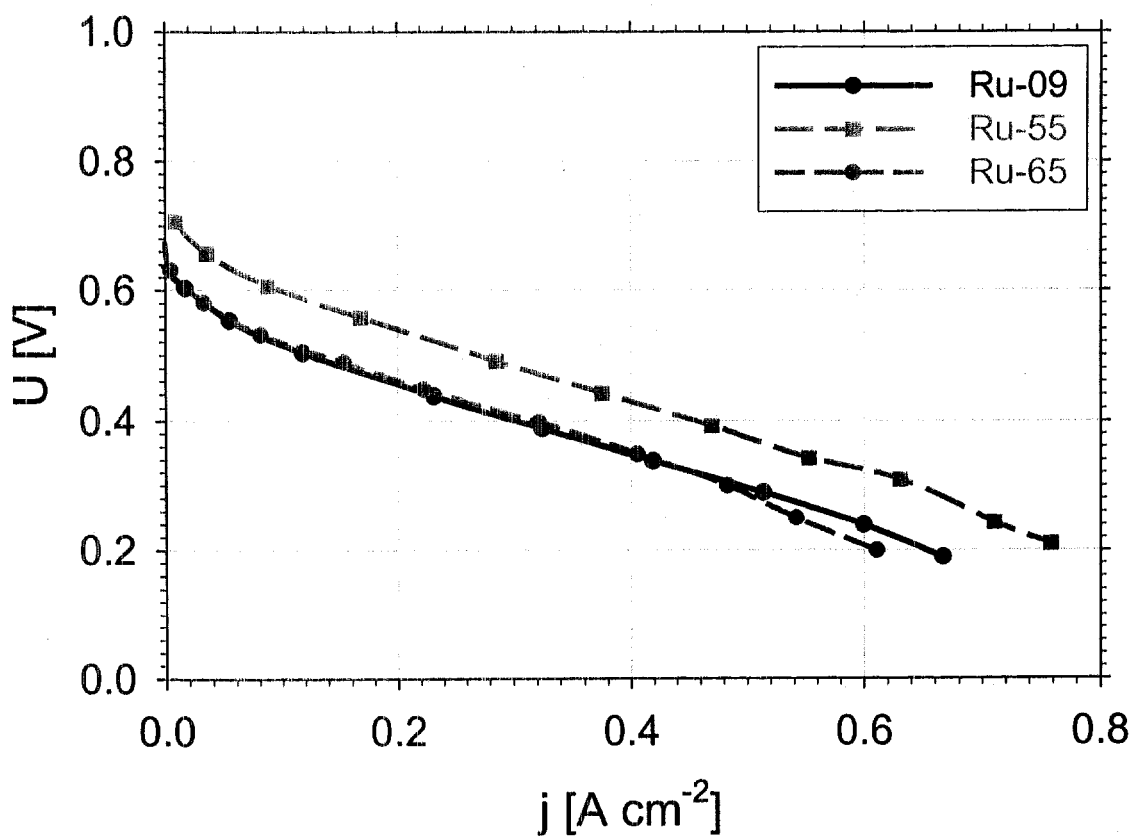
Figure 1 Hydrogen air performance of MEAs with three selected Pt-Ru anode catalysts at 80°C. Pt-Ru anode: H_2, 2.8 atm, ~9 mg cm^{-2} Pt-Ru; Pt cathode: air, 2.8 atm, ~6 mg cm^{-2} Pt.
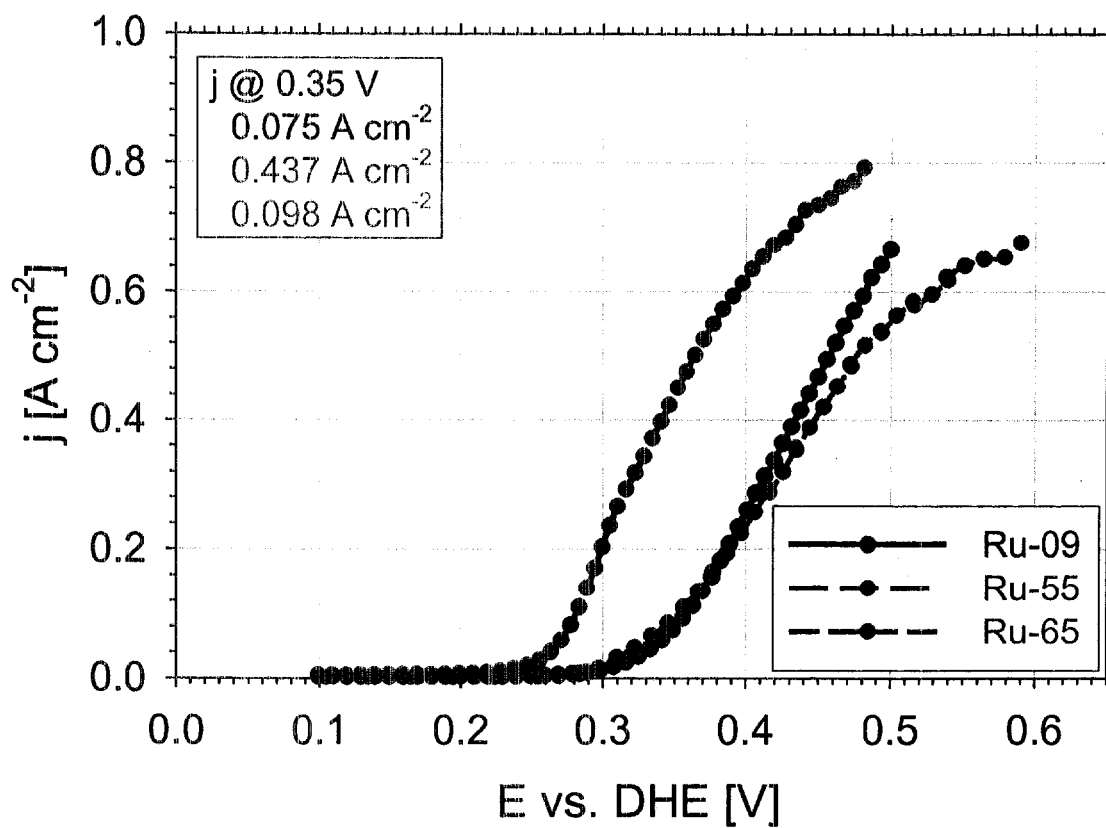
Figure 2 H_2-air performance at 0.7 V *vs.* bulk atomic percent of Ru in the anode catalyst. Test conditions as in Figure 1.
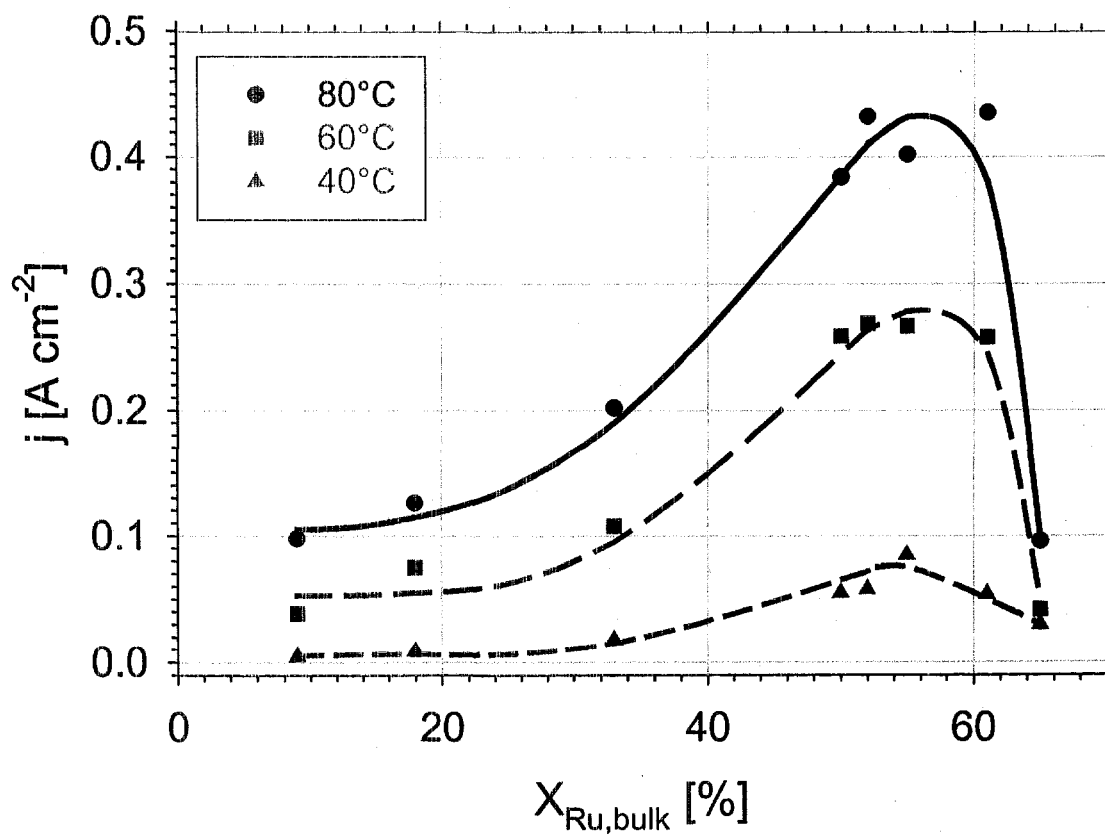
Figure 3 DMFC polarization plots for MEAs with three selected Pt-Ru anode catalysts at 80°C. Pt-Ru anode: 1.0 M MeOH, ~9 mg cm^{-2} Pt-Ru; Pt cathode: air, 2.8 atm, ~6 mg cm^{-2} Pt.
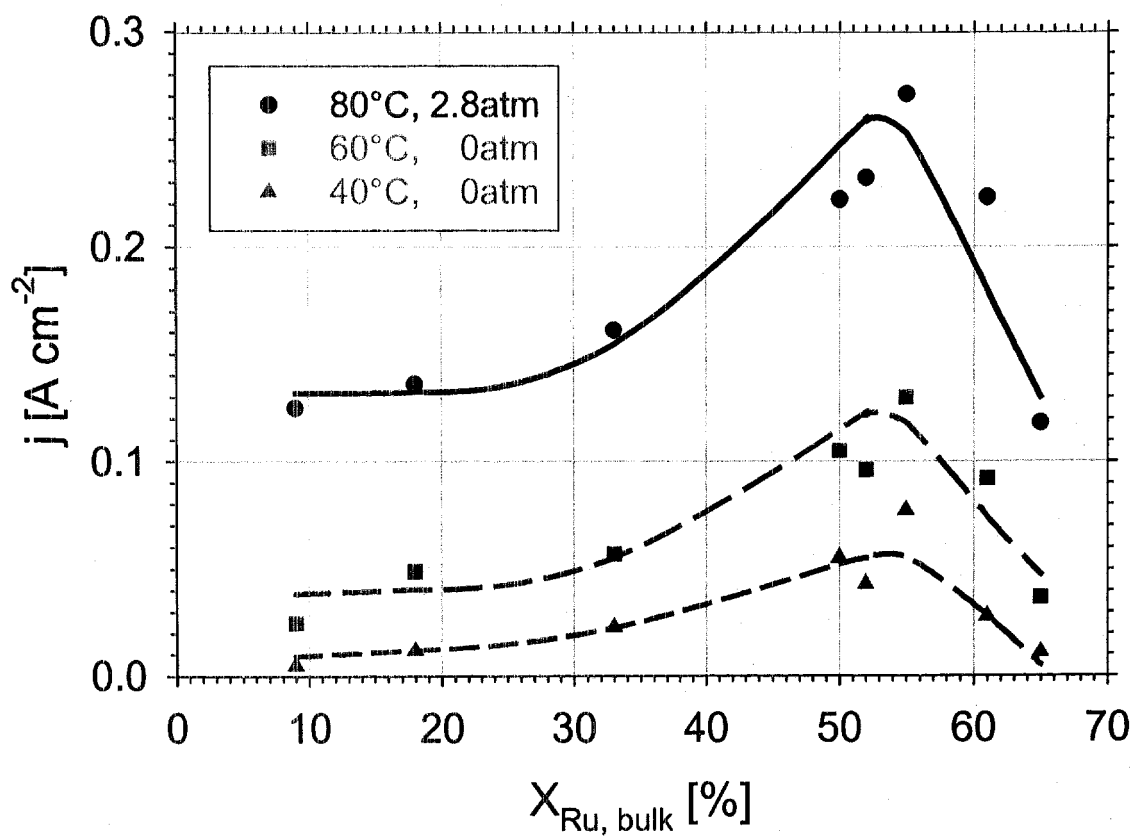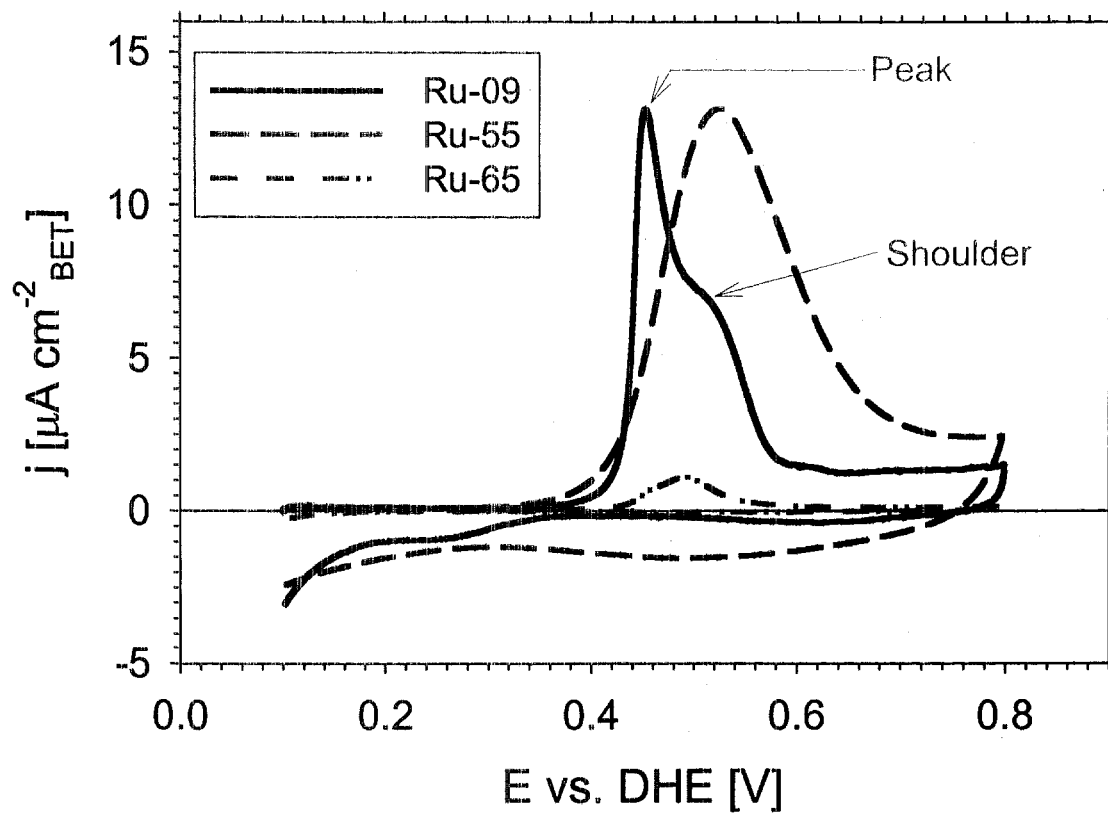
Figure 4 DMFC performance at 0.5 V *vs.* bulk atomic percent of Ru in the anode catalyst. Test conditions as in Figure 3.
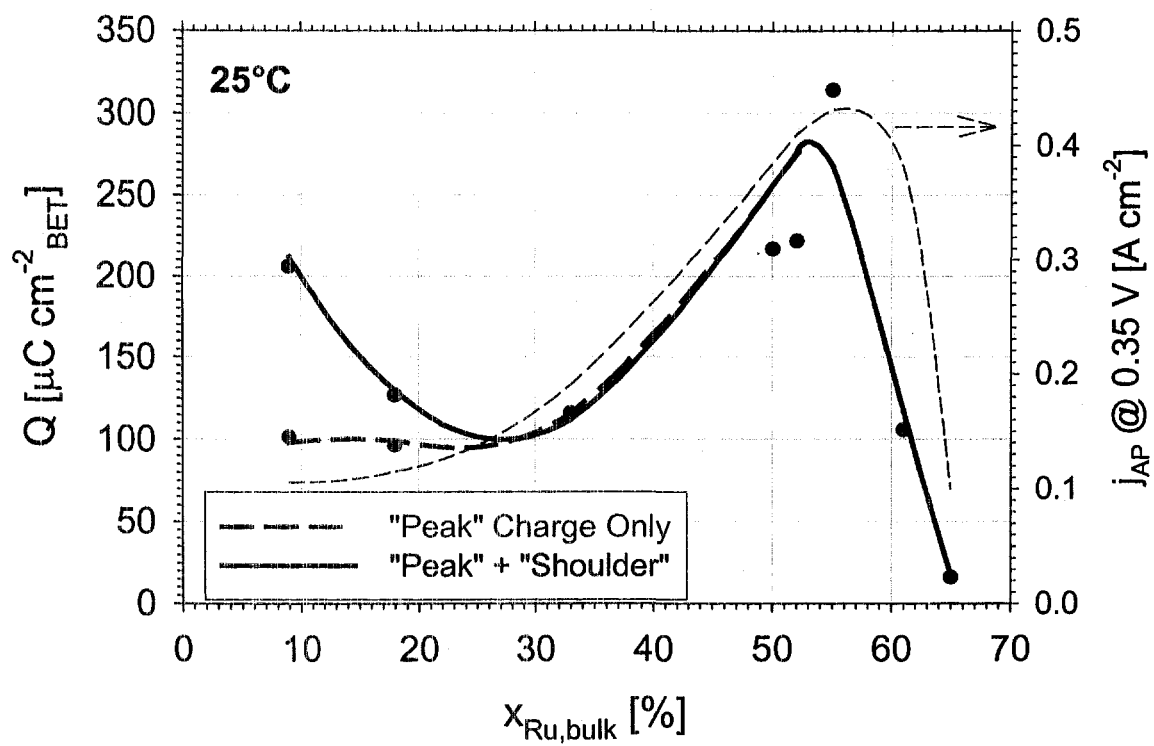
Figure 5 *iR*-corrected anode polarization plots at 80°C; 1.0 M MeOH.

Figure 6 Anode activity at 0.35 V *vs.* bulk atomic percent of Ru in the anode catalyst at three different cell temperatures; *iR*-corrected data; 1.0 M MeOH.
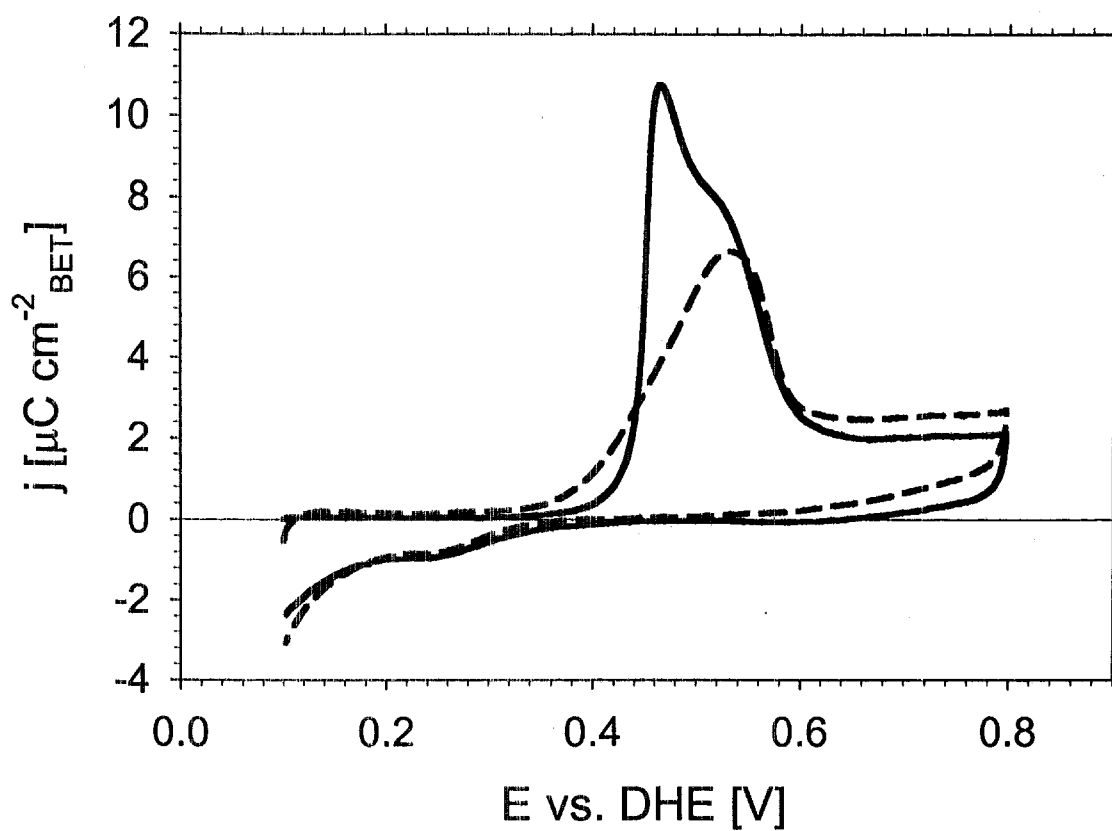
Figure 7 Voltammetric stripping of CO chemisorbed from the gas phase on three selected Pt-Ru catalysts at 0.1 V for 10 min; temperature 25°C; scan rate 5 mV s^{-1}.
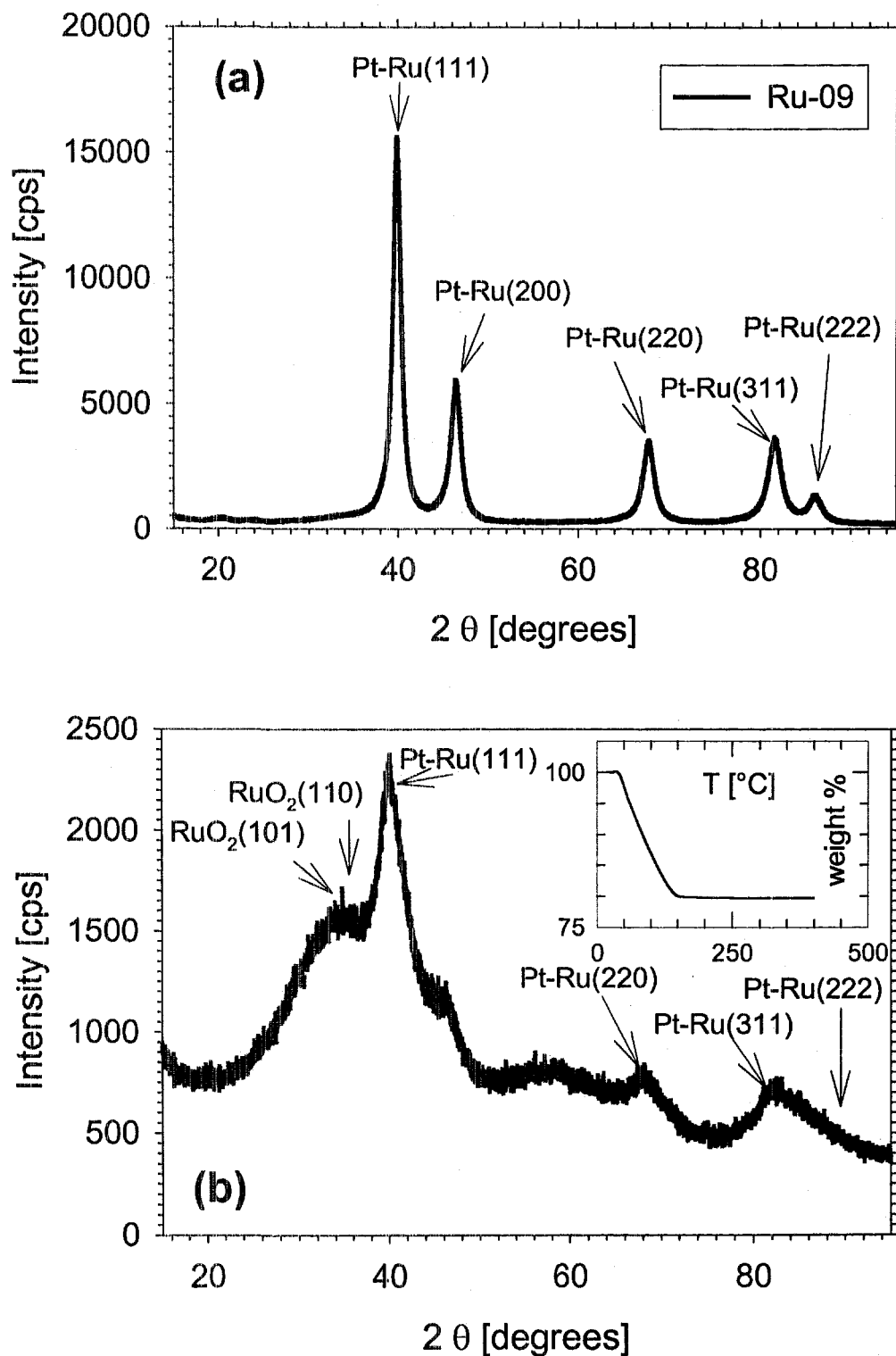
Figure 8 CO stripping charge *vs.* bulk atomic percent of Ru in the anode catalyst; test conditions as in Figure 7.

Figure 9 Comparison of stripping voltammetry (*iR*-corrected) of CO chemisorbed from the gas phase at 0.1 V for 10 min (solid line) and from 1.0 M aqueous MeOH at 0.1 V for 60 min (dashed line); temperature 25°C; scan rate 5 mV s^{-1}.

Figure 10 XRD traces from 15 to 96 degrees two-theta using CuK$_{\alpha 1}$ radiation of the "as-received" Johnson Mattey Ru-09 and Ru-65 catalysts. The indexed FCC alloy peaks and those for RuO$_2$ are labeled accordingly; **(a)** Ru-09, **(b)** Ru-65 with a TGA spectrum shown as an insert.

REFERENCES

1. H. A. Gasteiger, N. Marković, P. N. Ross, Jr. and E. J. Cairns, *J. Phys. Chem.* **97**, 12020 (1993).
2. H. N. Dinh, X. Ren, F. H. Garzon, P. Zelenay and S. Gottesfeld, *J. Electroanal. Chem.* **491**, 222 (2000).
3. M. Watanabe and S. Motoo, *J. Electroanal. Chem.* **60**, 275 (1975).
4. T. Iwasita, H. Hoster, A. John-Anacker, W. F. Lin and Vielstich; W., *Langmuir* **16**, 522 (2000).
5. S. C. Thomas, X. Ren, S. Gottesfeld and P. Zelenay, *Electrochim. Acta*, in press.
6. M. Watanabe, M. Uchida and S. Motoo, *J. Electroanal. Chem.* **229**, 395 (1987).
7. W. B. Wang, M. S. Zei and G. Ertl, *Phys. Chem. Chem. Phys.* **3**, 3307 (2001).
8. H. A. Gasteiger, N. Marković, P. N. Ross, Jr. and E. J. Cairns, *J. Electrochem. Soc.* **141**, 1795 (1994).